Approaching the Precipitation Temperature of the Deposition Solution and the Effects on the Internal Order of Polyelectrolyte Multilayers

Manesh Gopinadhan,[†] Heiko Ahrens,[†] Jens-Uwe Günther,[†] Roland Steitz,[‡] and Christiane A. Helm*,[†]

Institut für Physik, Ernst-Moritz-Arndt Universität, F.-L.-Jahn-Strasse 16, 17487 Greifswald, Germany, and Hahn-Meitner Institut, Glienicker Strasse 100, D-14109 Berlin, Germany

Received November 26, 2004; Revised Manuscript Received March 22, 2005

ABSTRACT: Polyelectrolyte multilayers are prepared by consecutively adsorbing poly(allylamine hydrochloride) (PAH) and poly(styrene sulfonate) (PSS) from aqueous KCl solution (1 mol/L) at different temperatures, approaching the precipitation temperature at 55 °C. The films are characterized by X-ray and neutron reflectometry, using selectively deuterated PSS layers. When the preparation solution is heated, the film thickness increases up to 75%; the film/air and the internal roughness increase by up to a factor of 3. Below 35 °C preparation temperature, the internal roughness is about 40% of the thickness of a polycation/polyanion layer pair, the same result as obtained when the bilayer thickness is controlled by varying the salt content in the deposition solution. At higher preparation temperatures, the interpenetration is more pronounced, a feature which may be attributed to the theoretically predicted changes of the polymer conformation in solution from extended configuration to pearl-necklace or even globular structures.

Introduction

Self-assembly processes of polyelectrolytes involving electrostatic interactions can be used to build up multilayered materials with unique properties. The basic principle is the sequential adsorption of positively and negatively charged polyelectrolytes.[1,2] Because polymers are typically flexible molecules, the resulting superlattice structures have somewhat fuzzy architectures. This leads to a behavior being dominated by internal interfaces and local interactions, differing largely from the corresponding volume material properties.

For many polyelectrolytes, the thickness of a polycation/polyanion pair within a polyelectrolyte multilayer is mainly determined by electrostatic interactions.[3,4] On increase of the salt concentration in the deposition solution, the thickness of a layer pair increases, a feature which is attributed to the screening of the electrostatic force during the deposition process.[2] However, secondary forces like polymer/solvent interaction or hydration forces are also found to influence the coverage and conformation of an adsorbing polyelectrolyte[4−6] even though the hierarchy of interactions and their respective influence is far from clear. We want to probe the influence of polymer/solvent interaction. By approaching the precipitation temperature of the polyelectrolyte, the polymer/solvent interaction can be tuned in a controlled way from good to bad to very bad.

The segment distribution of a polyelectrolyte layer within a mulitilayer is broader than its thickness,[1,7] the interdigitation is large enough to result in a constant monomer density, both for polycations and polyanions. Therefore, the stability of polyelectrolyte multilayers has been explained by the formation of local ion contact pairs,[8] both between monomers from adjacent and nonadjacent oppositely charged polyelectrolyte layers.

With the polyanion/polycation pair which was investigated most often (cf. Scheme 1), polystyrene (sulfonate) (PSS) and poly(allylamine hydrochloride) (PAH) the layer thickness and the layer interpenetration have been investigated systematically for different NaCl concentrations in the deposition solution.[7,9] Thus, it was possible to increase d_{bl}, the thickness per deposited polyelectrolyte bilayer, by 1 order of magnitude, from 6.5 Å (salt free) to 66 Å (3 M NaCl). However, the layer interpenetration as evidenced by neutron reflectivity remains constant. The interface roughness σ_{int} between adjacent polyelectrolyte layers increases roughly linearly with the thickness d_{bl} of a polyelectrolyte bilayer pair, $\sigma_{int} \approx 0.4 d_{bl}$.

Scheme 1. Molecular Structure of the Poly(ethylenimine) (PEI), Polystyrene Sulfonate (PSS) and Poly(allylamine hydrochloride) (PAH)

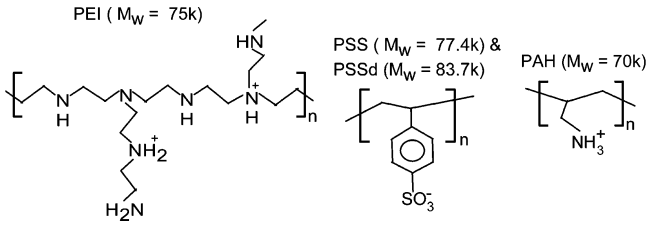

It is helpful to note that there are various theoretical studies on the conformations of polyelectrolytes in solution, where the electrostatic interaction strength is varied.[10,11] There, a crossover is found, from a dominating electrostatic interaction to the regime of strong screening, where the hydrophobic interactions dominate. During the crossover a multitude of structures is observed, transitions from an extended conformation to necklace like structures are predicted. While there are only few experiments characterizing the pearl-necklace structure in solution,[22] it has been observed when the polyelectrolyte has been adsorbed onto a surface.[12] To vary solvent/polyelectrolyte interaction, the deposition temperature is changed. The deposition solution contains 1 M KCl. This salt is selected instead of NaCl, because preiciptiation occurs at 55−60 °C. Thus, we can adjust the solvent conditions from good to bad. We found

[†] Ernst-Moritz-Arndt Universität.
[‡] Hahn-Meitner Institut.

10.1021/ma047552c CCC: $30.25
Published on Web 05/13/2005

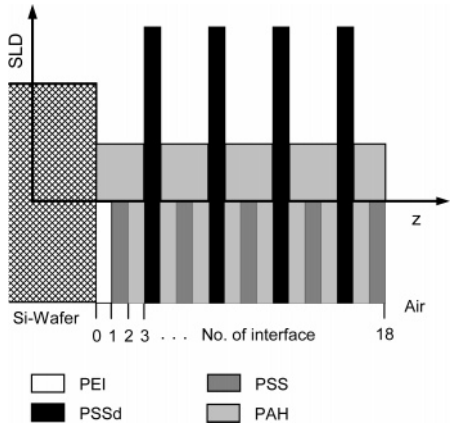

Figure 1. Schematic of architecture and resulting scattering length density profile of the polyelectrolyte multilayer PEI/PSS(PAH/PSSd/PAH/PSS)$_4$, assuming for simplicity zero internal roughness. Bottom section: layer sequence.

that the thickness per layer pair increases by a factor of about 1.5[6,13] if the temperature of the deposition solution is varied between 5 and 40 °C. The temperature dependent thickness increase can only be observed if deposition solutions with high salt concentrations are chosen, because it is necessary to screen both the amplitude and the range of the electrostatic interactions.[13,19] Actually, at our solvent conditions (1 M), the Debye screening length amounts to 3 Å, a length which corresponds to the diameter of a water molecule. Thus, the electrostatic and the monomer/solvent interaction can be assumed to have a similar (short) range.

To probe layer interpenetration by neutron reflectometry, polylectrolyte multilayers are prepared at different temperatures with selectively deuterated PSS-layers, i.e., PEI/PSS(PAH/PSSd/PAH/PSS)$_4$ (cf. Figure 1). Thus, we create a superstructure consisting of deuterated layers, which causes Bragg peaks in neutron reflectivity measurements. The peak position, width, and intensity are used to calculate the internal roughness σ_{int}.

Materials and Methods

Silicon wafers (generous gift of Wacker, Burghausen) serve as negatively charged substrates. The branched polycation poly(ethylene imine) (PEI; $M_w = 75$ kDa; Aldrich) has proved to be an efficient first layer, the polycation PAH ($M_w = 70$ kDa; Aldrich) is used for all subsequent layers. Polyanions are PSS ($M_w = 77.4$ kDa; PSS, Polymer Standard Service, Mainz, Germany) and deuterated PSSd ($M_w = 83.7$ kDa; PSS, Polymer Standard Service, Mainz, Germany). Ultrapure water was from Millipore (Milli-Q), KCl (99%) from Merck (Darmstadt, Germany).

For each adsorption step during polyelectrolyte multilayer buildup, the substrate is immersed for 30 min in a solution of 0.003 mol/L (monomer) polyelectrolyte and 1 M KCl and then washed in three beakers of clean water (soaking time 1 min each). All beakers are kept at the same temperature, which is adjusted externally by a thermostat (Haake, Germany). The films are prepared by a robot (Riegler&Kirstein, Berlin, Germany).

Small-angle X-ray reflectometry experiments are performed with a Seifert XRD 3003 TT diffractometer (Seifert, Germany) using Cu Kα radiation (wavelength $\lambda = 1.54$ Å). The neutron setup is experiment V6 at the Hahn-Meitner Institut, Berlin, Germany ($\lambda = 4.66$ Å). In these reflectivity experiments, the deviation $\delta = 1-n$ of the index of refraction n from 1 depends linearly on a material constant, which is directly related to the constituting molecules. For X-rays, this material constant is the electron density ρ ($\delta = \lambda^2/2\pi$ g ρr_o, with Thomson radius r_o). Similarly, for neutron optics, the scattering length density SLD $= \sum_i n_i b_i / \sum_i n_i V_i$ is the relevant parameter, with SLD as the ratio of the sum of the scattering lengths b_i and the molecular volumes V_i occurring in the system ($\delta = \lambda^2/2\pi \cdot$SLD).

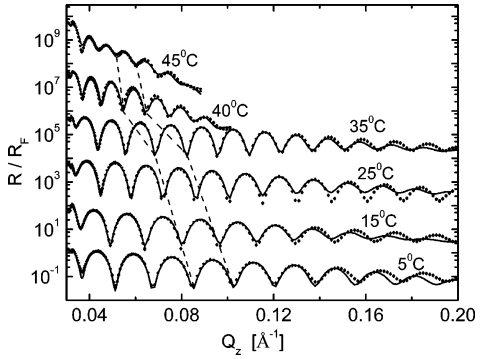

Figure 2. X-ray reflectivity curves normalized relative to the Fresnel reflectivity of films prepared from 1 M KCl solution at the temperatures indicated. For clarity, the reflectivity curves are shifted relative to each other. The dashed lines connect minima of equal order.

In both cases, n deviates only by $\approx 10^{-5}$ from 1. Therefore, approximations are possible, and the measured reflectivity R may be described as the Fresnel reflectivity R_F of an infinitely sharp interface modulated by interference effects from a thin surface layer.[14] Above about two critical angles of total external reflection ($\alpha_c = \sqrt{2\delta}$) the reflectivity is given by the kinematic approximation

$$\frac{R}{R_F} = \left|\frac{1}{\rho_{sub}}\int \rho'(z) e^{iQ_z z}\, dz\right|^2 \qquad (1)$$

ρ_{sub} is the electron density (or SLD, respectively) of the bulk phase, $\rho'(z)$ the gradient of the electron density (scattering length density, respectively) along the surface normal, and Q_z the wave vector transfer normal to the surface. The scattering length density profiles (electron density profiles, respectively) are calculated first by an indirect Fourier transform of the master formula.[15,16] Then, to quantify the molecular parameters, the exact, optical matrix formalism (dynamical approach) is used.[17,18]

The surface layer is parametrized as consisting of different slabs (each with a density and a thickness, as well as a roughness parameter). In all cases, the simulated reflectivity is convoluted with the angular divergence of the respective spectrometer (X-ray, 0.012°; neutrons, 0.017°).

Results

The X-ray reflectivity curves from polyelectrolyte multilayers prepared at different temperatures (cf. Figure 2) show many equidistant interference fringes. On increase of the preparation temperature, the distance between the minima narrows, indicating film thickening (the film thickness d is roughly proportional to the distance between two minima, $d = 2\pi/\Delta Q_z$). On increase of Q_z, the amplitude of the oscillation slowly decreases. From the decay, the film/air roughness $\sigma_{f/a}$ can be determined. At preparation temperatures above 30 °C, the decay is much more pronounced, indicating an increase of $\sigma_{f/a}$. Detailed data analysis reveals that $\sigma_{f/a}$ is almost constant (18.5 ± 1 Å) up to 30 °C, then one finds a sudden increase by about a factor three (cf. Figure 4).

The neutron reflectivity curves of the films previously characterized by X-ray reflectivity are shown in Figure 3. The first three interference fringes, so-called Kiessig fringes, measure the film thickness, similar to the X-ray reflectivity curves (cf. Figure 2). One finds that the film

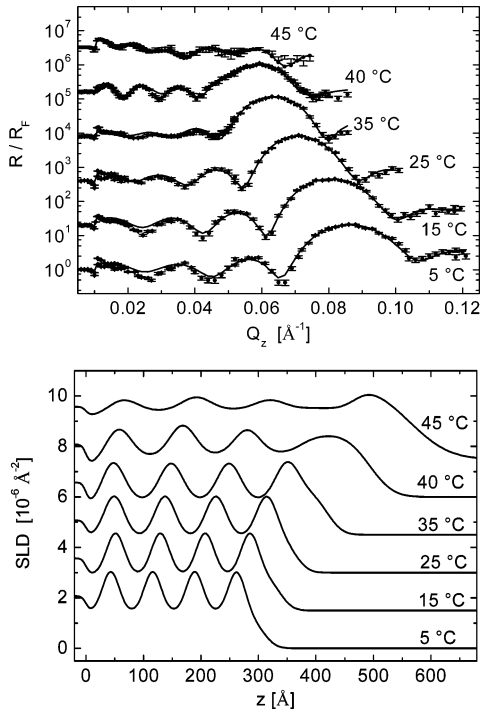

Figure 3. Top: Normalized neutron reflectivity curves from the same samples, from which the X-ray reflectivity curves shown in Figure 2 were obtained. For clarity, the reflectivity curves are shifted relative to each other. The lines are calculated from the scattering length density profiles shown in the bottom part, derived from the simple model.

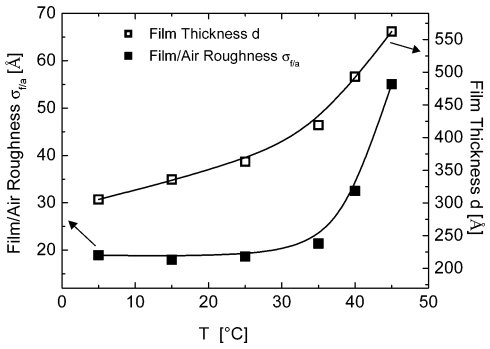

Figure 4. Film thickness d (open squares) from neutron and film/air roughness $\sigma_{f/a}$ (full squares) from X-ray reflectivity as a function of the deposition temperature.

thickness changes from 305 to 562 Å, i.e., by about 75%. Additionally, there is a Bragg peak due to the superstructure from the PSSd slabs. On increase of the preparation temperature a shift of the peak to smaller Q_z values is observed, indicative of a thickening of the repeat unit consisting of two polyelectrolyte bilayers. Unexpected is the decrease of the peak intensity at high preparation temperatures, which suggests a decreased contrast in the superstructure.

The scattering length densities of the respective molecules or monomers SLD_{xxx} are the quotient of the scattering length ($b^{PSS} = 472.03 \times 10^{-6}$Å, $b^{PSSd} = 1200.73 \times 10^{-6}$Å, $b^{PAH} = -6.32 \times 10^{-6}$Å, $b^{H_2O} = -16.75 \times 10^{-6}$Å) and the volume ($V_{PSS} = 200$ Å$^3 = V_{PSSd}$, $V_{PAH} = 97$ Å^3, $V_{H_2O} = 29.98$ Å^3). PEI is assumed to have the same monomer volume and scattering length density as PAH.

Let us start with finding a model to describe the neutron reflectivity data obtained from the films prepared at low temperatures. Assuming that one PAH monomer binds to one PSS monomer, the volume fraction of polyanion is 2:1 (since $V_{PSS} = 200$ Å$^3 \approx 2V_{PAH} = 194$ Å^3). Because of the constant mass density of the film, the thickness of a PSS-layer is double the one of a PAH-layer. Therefore, in a repetition unit consisting of two PSS and two PAH-layers, the thickness of the deuterated PSS-layer amounts to $^1/_3$ of the length of the repetition unit, the nondeuterated layers are $^2/_3$. Each repeat unit is described by three slabs of identical thickness, one for the deuterated PSSd-layer and two for the PAH/PSS/PAH-layers. Two additional slabs are necessary to describe the precursor polyelectrolyte layer adjacent to the Si wafer, and the air-adjacent outer layer. Thus, one obtains a 12-slab model, as listed in Table 1. However, there are very few free parameters in the fits: the roughness for the film/air and the substrate/film interfaces are taken from the fits to the X-ray reflectivity measurements, since the larger Q_z range of these measurements allows to quantify the decay of the oscillation amplitudes more reliably.

For the samples prepared at temperatures of 35 °C and below, the fits have only four free parameters: (1) the scattering length density of the PSSd-layer, (2) the scattering length density of the nondeuterated layers, (3) the thickness of the layer adjacent to the substrate, and (4) the thickness of a bilayer pair within a repeat unit. Some additional constraints are introduced, if possible, for the thickness and the scattering length densities of the slabs which describe the precursor layers next to the substrate and the air-adjacent outer layers. A further constraint concerns the internal roughness σ_{int} between adjacent slabs, which is set to half of the slab thickness. This constraint was found to be valid for polyelectrolyte multilayers when only the salt concentration in the deposition solution was varied.[7] The fact that very good fits can be obtained with such a simple model highlights its validity. Note that on increase of the temperature to 35 °C, the reflectivity curve is less regular and the deduced scattering length density profile slightly less modulated (cf. Figure 3).

More complicated to model are the measurements from the high temperature samples (cf. Figure 3), where the Bragg peak is very weak indicating increased layer interdigitation. Furthermore, the decay of the oscillations cannot be described by a simple roughness. The constraints for the slab thickness are maintained, and the scattering length density of the slabs describing the precursor and the outer layer are fit parameters, too. Unexpected is the finding that the scattering length density of the deuterated slabs varies slightly within the layer, a parabolic function is necessary to describe it (n is the slab number as given in Figure 1, or in Table 1 in the Appendix):

$$SLD_n = A + nB + n^2C, \quad n = 2, 5, 8, 11 \qquad (2)$$

The scattering length density of the nondeuterated slabs varies very little within the repeat units, and the variation can be described with a linear function

$$SLD_n = D + nE, \quad n = 3, 4, 6, 7, 9, 10 \qquad (3)$$

Summarizing, five strongly correlated parameters (A, B, C, D, E) are necessary to calculate the scattering length density of the repeat units.

The scattering length density profiles shown in Figure 3 are less structured if the films are prepared at temperatures above 35 °C. The scattering length density

Table 1. Parameters of the 12-Layer Slab Model Used to Fit the Neutron Reflectivity Curves of the Various Samples[a]

sample	Si wafer	PEI/PSS/PAH layer 1	PSSd layer 2 (deut.)	PAH/PSS/PAH layer 3 layer 6 layer 9	PAH/PSS/PAH layer 4 layer 7 layer 10	PSSd layer 5 layer 8 layer 11 (deut.)	PAH/PSS layer12	total film thickness
5 °C	$SLD_{Si} = 2.07$	$\mathbf{l_1 = 30.95}$ $\mathbf{SLD_1 = 1.47}$	$\mathbf{l_2 = 24.33}$ $\mathbf{SLD_2 = 3.76}$	$l_3 = l_6 = l_9 = l_2$ $SLD_3 = SLD_6 = SLD_9 = SLD_1$	$l_4 = l_7 = l_{10} = l_2$ $SLD_4 = SLD_7 = SLD_{10} = SLD_1$	$l_5 = l_8 = l_{11} = l_2$ $SLD_5 = SLD_8 = SLD_{11} = SLD_2$	$l_{12} = l_1$ $SLD_{12} = SLD_3$	$\Sigma l_i = 305.2$
	$\sigma_{0/1} = 6$	$\sigma_{1/2} = l_2/2$	$\sigma_{2/3} = l_2/2$	$\sigma_{3/4} = \sigma_{6/7} = \sigma_{9/10} = \sigma_{2/3}$	$\sigma_{4/5} = \sigma_{7/8} = \sigma_{10/11} = \sigma_{2/3}$	$\sigma_{5/6} = \sigma_{8/9} = \sigma_{11/12} = \sigma_{2/3}$	$\sigma_{f/a} = 18.96$	
15 °C	$SLD_{Si} = 2.07$	$\mathbf{l_1 = 38.36}$ $\mathbf{SLD_1 = 1.44}$	$\mathbf{l_2 = 26.00}$ $\mathbf{SLD_2 = 3.80}$	$l_3 = l_6 = l_9 = l_2$ $SLD_3 = SLD_6 = SLD_9 = SLD_1$	$l_4 = l_7 = l_{10} = l_2$ $SLD_4 = SLD_7 = SLD_{10} = SLD_1$	$l_5 = l_8 = l_{11} = l_2$ $SLD_5 = SLD_8 = SLD_{11} = SLD_2$	$l_{12} = l_1$ $SLD_{12} = SLD_3$	$\Sigma l_i = 336.7$
	$\sigma_{0/1} = 6$	$\sigma_{1/2} = l_2/2$	$\sigma_{2/3} = l_2/2$	$\sigma_{3/4} = \sigma_{6/7} = \sigma_{9/10} = \sigma_{2/3}$	$\sigma_{4/5} = \sigma_{7/8} = \sigma_{10/11} = \sigma_{2/3}$	$\sigma_{5/6} = \sigma_{8/9} = \sigma_{11/12} = \sigma_{2/3}$	$\boldsymbol{\sigma_{f/a} = 18.0}$	
25 °C	$SLD_{Si} = 2.07$	$\mathbf{l_1 = 34.2}$ $\mathbf{SLD_1 = 1.46}$	$\mathbf{l_2 = 29.5}$ $\mathbf{SLD_2 = 3.74}$	$l_3 = l_6 = l_9 = l_2$ $SLD_3 = SLD_6 = SLD_9 = SLD_1$	$l_4 = l_7 = l_{10} = l_2$ $SLD_4 = SLD_7 = SLD_{10} = SLD_1$	$l_5 = l_8 = l_{11} = l_2$ $SLD_5 = SLD_8 = SLD_{11} = SLD_2$	$l_{12} = l_1$ $SLD_{12} = SLD_3$	$\Sigma l_i = 363.4$
	$\sigma_{0/1} = 6$	$\sigma_{1/2} = l_2/2$	$\sigma_{2/3} = l_2/2$	$\sigma_{3/4} = \sigma_{6/7} = \sigma_{9/10} = \sigma_{2/3}$	$\sigma_{4/5} = \sigma_{7/8} = \sigma_{10/11} = \sigma_{2/3}$	$\sigma_{5/6} = \sigma_{8/9} = \sigma_{11/12} = \sigma_{2/3}$	$\sigma_{f/a} = 18.70$	
35 °C	$SLD_{Si} = 2.07$	$\mathbf{l_1 = 30.55}$ $\mathbf{SLD_1 = 1.21}$	$\mathbf{l_2 = 35.59}$ $\mathbf{SLD_2 = 3.48}$	$l_3 = l_6 = l_9 = l_2$ $\mathbf{SLD_3 = 1.39}$ $SLD_6 = SLD_9 = SLD_3$	$l_4 = l_7 = l_{10} = l_2$ $SLD_4 = SLD_7 = SLD_{10} = SLD_3$	$l_5 = l_8 = l_{11} = l_2$ $SLD_5 = SLD_8 = SLD_{11} = SLD_2$	$\mathbf{l_{12} = 52.66}$ $\mathbf{SLD_{12} = 1.77}$	$\Sigma l_i = 439.1$
	$\sigma_{0/1} = 6$	$\sigma_{1/2} = l_1/2$	$\sigma_{2/3} = l_2/2$	$\sigma_{3/4} = \sigma_{6/7} = \sigma_{9/10} = \sigma_{2/3}$	$\sigma_{4/5} = \sigma_{7/8} = \sigma_{10/11} = \sigma_{2/3}$	$\sigma_{5/6} = \sigma_{8/9} = \sigma_{11/12} = \sigma_{2/3}$	$\sigma_{f/a} = 21.4$	
40 °C	$SLD_{Si} = 2.07$	$l_1 = l_2$ $\mathbf{SLD_1 = 1.24}$	$\mathbf{l_2 = 37.36}$ $\mathbf{SLD_2 = 3.32}$	$l_3 = l_6 = l_9 = l_2$ $\mathbf{SLD_3 = 1.62}$ $\mathbf{SLD_6 = 1.68}$ $\mathbf{SLD_9 = 1.74}$	$l_4 = l_7 = l_{10} = l_2$ $\mathbf{SLD_4 = 1.64}$ $\mathbf{SLD_7 = 1.70}$ $\mathbf{SLD_{10} = 1.76}$	$l_5 = l_8 = l_{11} = l_2$ $\mathbf{SLD_5 = 3.26}$ $\mathbf{SLD_8 = 3.56}$ $\mathbf{SLD_{11} = 4.22}$	$\mathbf{l_{12} = 85.74}$ $\mathbf{SLD_{12} = 2.48}$	$\Sigma l_i = 496.7$
	$\sigma_{0/1} = 6$	$\sigma_{1/2} = l_2/2$	$\sigma_{2/3} = l_2/2$	$\sigma_{3/4} = \sigma_{6/7} = \sigma_{9/10} = \sigma_{2/3}$	$\sigma_{4/5} = \sigma_{7/8} = \sigma_{10/11} = \sigma_{2/3}$	$\sigma_{5/6} = \sigma_{8/9} = \sigma_{11/12} = \sigma_{2/3}$	$\sigma_{f/a} = 32.5$	
45 °C	$SLD_{Si} = 2.07$	$l_1 = l_2$ $\mathbf{SLD_1 = 1.23}$	$\mathbf{l_2 = 42.61}$ $\mathbf{SLD_2 = 2.9}$	$l_3 = l_6 = l_9 = l_2$ $\mathbf{SLD_3 = 1.9}$ $\mathbf{SLD_6 = 1.96}$ $\mathbf{SLD_9 = 2.02}$	$l_4 = l_7 = l_{10} = l_2$ $\mathbf{SLD_4 = 1.92}$ $\mathbf{SLD_7 = 1.98}$ $\mathbf{SLD_{10} = 2.04}$	$l_5 = l_8 = l_{11} = l_2$ $\mathbf{SLD_5 = 2.62}$ $\mathbf{SLD_8 = 2.83}$ $\mathbf{SLD_{11} = 3.4}$	$\mathbf{l_{12} = 93.42}$ $\mathbf{SLD_{12} = 2.97}$	$\Sigma l_i = 562.1$
	$\sigma_{0/1} = 6$	$\sigma_{1/2} = l_2/2$	$\sigma_{2/3} = l_2/2$	$\sigma_{3/4} = \sigma_{6/7} = \sigma_{9/10} = \sigma_{2/3}$	$\sigma_{4/5} = \sigma_{7/8} = \sigma_{10/11} = \sigma_{2/3}$	$\sigma_{5/6} = \sigma_{8/9} = \sigma_{11/12} = \sigma_{2/3}$	$\sigma_{f/a} = 55.07$	

[a] Free parameters are indicated by bold type; for all other parameters, the constraints are given. Any scattering length density (SLD) is given in 10^{-6} Å^{-2}, thickness (l_x) and roughness (σ_x) in Å.

maxima due to the deuterated PSS-layers decrease in amplitude and the background due to the nondeuterated slabs is higher. These features suggest more pronounced interdigitation at higher preparation temperatures. To determine the interface roughness σ_{int} independent of the thickness of a repeat unit, the scattering length density profiles have to be quantified in terms of molecular parameters. With this approach, one can also take the more pronounced interpenetration into account, which elevates the measured scattering length density of the PAH/PSS/PAH layers within a repeat unit, and correspondingly decreases the one of the PSSd layer.

As a first step, the film composition, i.e., the water content, has to be quantified. The number of water molecules per PAH/PSS monomer pair is calculated from the average scattering length density, SLD_{av}, integrated along the surface normal

$$SLD_{av} = \frac{1}{l_{repeat\ unit}} \int_{repeat\ unit} SLD(z)dz \qquad (4)$$

Assuming that the film consists only of pairs of oppositely charged monomers, and of water molecules, SLD_{av} can be calculated according to

$$SLD_{av} = \frac{b^{PSS} + b^{PSSd} + 2b^{PAH} + n_{H_2O} b^{H_2O}}{2V_{PSS} + 2V_{PAH} + n_{H_2O} V_{H_2O}} \qquad (5)$$

with n_{H_2O} as the number of water molecules. Simple algebra yields the number of water molecules per monomer pair, $n_{H_2O}/(V_{PSS} + V_{PAH})$. The obtained water incorporation amounts to about 2 water molecules per monomer pair, well in agreement with the literature.[9]

The water content is a rather reliable parameter, since it mainly influences the amplitude of the Kiessig oscillations in the neutron reflectivity curves. In the experiments shown in Figure 2, SLD_{av} is above the one of the Si wafer. Therefore, an increase in the water concentration (with its negative SLD) would cause the mean film scattering length density SLD_{av} to be identical to the one of the substrate. Then, there would be no contrast from the substrate/film interface, and there would be no Kiessig oscillations (see also Figure 3, bottom and Figure 6). This argument is only qualitatively correct, for quantitative agreement one has also to consider interference from the selectively deuterated layers. Actually, changing the water content by 10% and allowing all other parameters to adjust changes χ^2 by 10%.

Considering the actual scattering length density profiles derived from the neutron scattering data (cf. Figure 3), the deuterated PSSd layers can be recognized, they resemble bell curves. Obviously, there is substantial interpenetration between the consecutively deposited layers. The height of the bell curves (i.e., the contrast) is constant up to 35° preparation temperature, then it decreases, indicating an increase of the internal roughness.

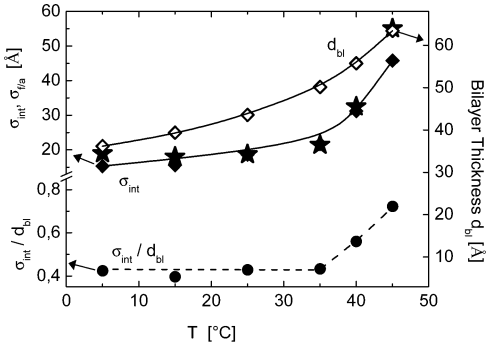

Figure 5. Thickness per bilayer pair d_{bl} (open diamonds) and internal roughness σ_{int} (full diamonds), together with the quotient σ_{int}/d_{bl} (full circles). For comparison, also the film/air roughness $\sigma_{f/a}$ is shown (stars).

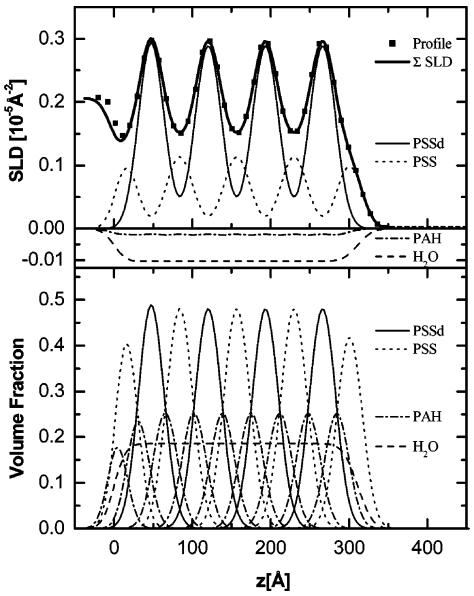

Figure 6. Top: Scattering length density profile of the sample prepared at 5 °C, as obtained with the simple model from the neutron reflectivity data (full squares) and calculated from the molecular model (bright line, ΣSLD). In the latter, the scattering length density is calculated as the sum of the profiles of the constituting layers (PSS, PSSd, and PAH), assuming homogeneous water incorporation. Bottom: The volume fraction profile corresponding to the scattering length density profile as calculated with the molecular model.

To describe the scattering length density profile with a molecular model, we need to take each deposited polyelectrolyte layer into account:

$$\mathrm{SLD}(z) = v_{\mathrm{Si}}(z)\cdot\mathrm{SLD}_{\mathrm{Si}} + v_{\mathrm{H_2O}}(z)\cdot\mathrm{SLD}_{\mathrm{H_2O}} + v_{\mathrm{PAH}}(z)\cdot\mathrm{SLD}_{\mathrm{PAH}} + v_{\mathrm{PSS}}(z)\cdot\mathrm{SLD}_{\mathrm{PSS}} + v_{\mathrm{PSSd}}(z)\cdot\mathrm{SLD}_{\mathrm{PSSd}} \quad (6)$$

v_x describes the volume fraction of the respective molecules along the surface normal.

The nth polyelectrolyte layer is given by ($n = 4,5, \ldots 17$; for layers at the edges some adjustments are necessary, details in the Appendix):

$$\mathrm{SLD}_{\mathrm{layer}.n} = A(n)\left(\mathrm{erf}\left(\frac{z - z_n}{\sigma_{\mathrm{int}}}\right) - \mathrm{erf}\left(\frac{z - z_{n+1}}{\sigma_{\mathrm{int}}}\right)\right) \quad (7)$$

$A(n)$ is the scattering length density after taking water incorporation into account. The error function describes the scattering length density gradient of a layer of thickness $z_{n+1} - z_n$, σ_{int} is a measure of the width of the gradient region.

If the internal roughness σ_{int} would be close to zero, then the layers would be stratified, as sketched in Figure 1. The deuterated layers would protrude from the polyelectrolyte multilayer with its constant scattering length density (we assume homogeneous distribution of both water and PAH). Because of the absence of interpenetration, the changes in scattering length density within the film would amount to $\mathrm{SLD_{PSSd}} - \mathrm{SLD_{PSS}}$, providing maximum contrast for the neutron reflectivity measurements. If the internal roughness exceeds the layer thickness by about a factor of 0.5, i.e., $\sigma_{int} \geq (1/2)(z_{n+1} - z_n)$, the profile of the deuterated layer resembles a bell curve. This is the case of our experiments. On further increase of σ_{int}, the layer interpenetration gets more pronounced. This causes a decrease in contrast in the scattering length density profiles, eventually the scattering length density within the film would be constant. Since in Figure 3, a decrease of contrast in the scattering length density profiles is observed, if the polyelectrolyte multilayers were prepared at temperatures above 35 °C, one might conclude that both σ_{int} and the ratio σ_{int}/d_{bl} increase.

With this molecular model (described in detail in the Appendix) five free parameters are necessary to describe a scattering length density profile, (i) the average water content α, (ii) the internal roughness σ_{int}, and (iii) the average thickness per polyelectrolyte bilayer d_{bl}, as well as (iv) the average thickness of a precursor layer $l_{\mathrm{precursor.av}}$ and (v) of an outer layer $l_{\mathrm{outer.av}}$. The water content α agrees very well with the value calculated from $\mathrm{SLD_{av}}$ according to eq 5 (cf. Table 2).

In Figure 6, for one sample the scattering length density as obtained from the neutron reflectivity curve is shown together with the one derived from the molecular model. Within the polyelectrolyte multilayer the agreement is very good, deviations occur at the substrate/film and the film/air interface. As shown in Figure 5, the increase of the bilayer thickness d_{bl} with the deposition temperature is roughly proportional to the film thickness, indicating that the precursor and outer layers have only minor influence on the multilayer buildup, as expected.[1] Also, the internal roughness increases with the deposition temperature. Up to 35 °C, we find $\sigma_{int}/d_{bl} \cong 0.4$. However, approaching the precipitation temperature, the increase of the internal roughness is more pronounced, actually the ratio σ_{int}/d_{bl} almost doubles. A sketch of the polyelectrolyte multilayer composition prepared at different temperatures is shown in Figure 7.

Discussion

On increasing the deposition temperature, the thickness per polyelectrolyte bilayer increases by 70%, from ~36 to 63 Å. Simultaneously, the internal roughness σ_{int} changes by a factor three, from ~15 to ~45 Å. It is intriguing to observe that up to 35 °C, we find $\sigma_{int}/d_{bl} \cong 0.4$ in quantitative agreement with earlier experiments,[7,9] when the polyelectrolyte bilayer thickness was varied by a factor of 10 by adjusting the salt concentration within the deposition solution. This finding strongly promotes the suggestion given originally by Tan et al.[19] that heat affects the polyelectrolyte films in a manner similar to added salt. Added salt swells the film by screening the amplitude of the electrostatic forces which bind the film together. Similarly, high-temperature

Table 2. Water Molecules per Monomer Pair Calculated from the Average Scattering Length Density and from the Stratified Molecular Layer Model[a]

T (°C)	N_{H_2O}/PAH−PSS monomer pair (calculated from molecular model)	N_{H_2O}/PAH−PSS monomer pair (calculated from simple model)	total film thickness d (Å)	thickness per bilayer pair (Å)	thickness of precursor and outer bilayer (Å)
5	1.99	2.27	305.2	36.1	20.63/30.95
15	1.98	2.23	336.0	39.0	25.57/38.36
25	2.07	2.00	363.4	43.6	22.8/34.2
35	2.62	2.45	419.1	50.2	20.37/52.66
40	2.35	2.20	493.3	55.7	24.9/85.74
45	2.33	2.35	562.1	63.4	28.4/93.42

[a] Also given is the total film thickness, as well as the thickness per polyelectrolyte bilayer pair and the mean thickness of the precursor and outer layer.

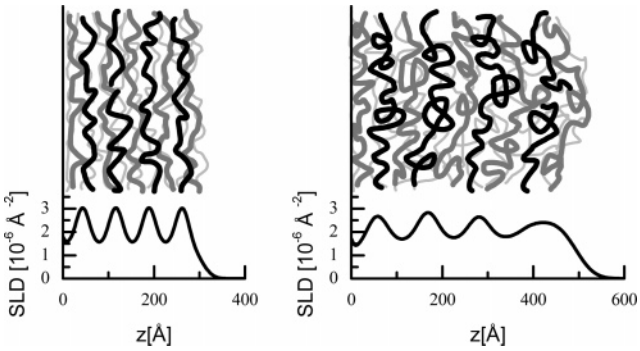

Figure 7. Schematic of contrast decrease due to larger layer interpenetration caused by polyelectrolytes adsorbing in a pearl-necklace or a partly globular structure. Same color code as in Figure 1, bottom.

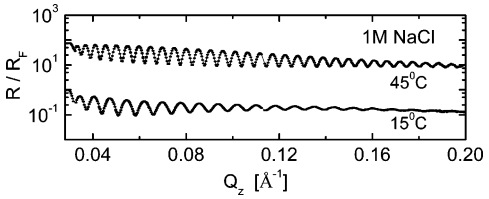

Figure 8. X-ray reflectivity curves normalized relative to the Fresnel Reflectivity of films prepared from 1 M NaCl solution at the temperatures indicated. For clarity, the reflectivity curves are shifted relative to each other.

promotes localized dissociation and increased conformational dynamics. The salt decreases barriers such conformational changes whereas the increased temperature provides the kinetic energy necessary to surmount the barriers. The addition of 1 M salt reduces the Coulombic contribution to conformational barriers so that the total energy barrier (which is the sum of steric, Coulombic and secondary interactions) is not too large compared to kT. Under a simple Arrhenius model, the rates of conformational change should depend exponentially on the ratio between the barrier height ΔE and T. This model is consistent with the fact that the ionic strength dependence is much stronger than the temperature dependence, i.e., increasing the salt from 0.1 to 1 M salt changes the film thickness by a factor of 10, whereas varying the temperature by 20% changes it by about a factor of 2.[19]

It is interesting to note that the film/air roughness $\sigma_{f/a}$ almost coincides with σ_{int}, cf. Figure 5. In some cases, $\sigma_{f/a}$ slightly exceeds σ_{int}, at most by 20%. This agreement suggests that the roughness of both the internal interfaces and the film/air interface can be attributed to the same physical origin. Similarly, a large film/air roughness may be an indication of large internal roughness. Similar changes in the thickness per polyelectrolyte bilayer on increase of the deposition temperature have also been observed with other monovalent salts like NaCl in solution, there the deposition temperature could be increased even further, because no precipitation occurs.[19] Our own X-ray experiments corrobate these findings, furthermore we do not find any increase in the film/air roughness; cf. Figure 8.

However, for films prepared from KCl solution, the pronounced increase in the internal roughness as well as the film/air roughness are induced in the vicinity of the precipitation temperature. As the precipitation temperature of the polyelectrolyte solution is approached, the polymer/solvent interaction deteriorates. Both analytical calculations (i.e., scaling models) and off-lattice Monte Carlo simulations of the conformations of polyelectrolytes in poor solvent find that there is a range of temperatures and charge densities for which the polymer has a necklacelike shape with compact beads joined by narrow strings (pearl-necklace model).[10,11,20,23] With changes in the temperature or decrease of polymer charge, the polyelectrolyte chain is expected to undergo a cascade of transitions from extended structure to a pearl necklaces, a pearl necklace to a cylinder, and a cylinder to a coil. In particular, it is calculated that hydrophobic polyelectrolytes exhibit a large variety of conformations compared to flexible or semiflexible polyelectrolytes without hydrophobic groups.[11]

There are various experiments which appear to be in agreement with these findings. Studies of the behavior of a solvophobic polyelectrolyte in a series of polar organic solvents of various quality and polarity with small-angle X-ray scattering found qualitative agreement with the scaling predictions for the radius of gyration.[10,21] These different conformations in solution are likely to be related to the conformation of adsorbed polyelectrolytes, as revealed by AFM studies. For instance, if the polyelectrolyte charge is tuned through the solution pH, for a highly charged polyelectrolyte, an extended coil conformation is observed. When the pH is increased, the polyelectrolyte charge decreases and induces a segmental collapse through pearl-necklace structures. At large pH, one can observe a globular conformation.[12]

If polyelectrolyte multilayers are prepared from charged polymers with hydrophobic backbones at conditions approaching precipitation, one might conclude that the polyelectrolytes adsorb not only in a flat conformation but also partly in a coil or globule conformation. Obviously, the conformation within the globules is rather loose, contact ion pairs are still formed. Also, the electrostatic and entropic froces which determine how much polyelectrolyte is adsorbed still dominate the

polyelectrolyte multilayer buildup. However, the closer one gets to precipitation conditions, the more pearls or globules are found within an adsorbed polyelectrolyte layer, thus the internal roughness is increased, as well as the film/air roughness.

Conclusion

Polyelectrolyte multilayers are prepared by consecutively adsorbing poly(allylamine hydrochloride) (PAH) and polystyrene sulfonate (PSS) from aqueous KCl solution (1 mol/L) at different temperatures, approaching the precipitation temperature at 55 °C. The films are characterized by X-ray and neutron reflectometry, using selectively deuterated PSS layers. On heating the preparation solution, the film thickness increases by up to 70%, the film/air and the internal roughness by up to a factor of 3 (the latter are identical within 20%). Up to 35 °C preparation temperature, the internal roughness is about 40% of the thickness of a polycation/polyanion layer pair, the same result as obtained when the bilayer thickness is controlled by varying the salt content in the deposition solution. At higher preparation temperatures, the interpenetration is more pronounced, a feature which may be attributed to the theoretically predicted changes of the deposition solution from extended configuration to pearl-necklace or even globular structures.

Acknowledgment. We gratefully acknowledge the support of Hahn-Meitner-Institut Berlin with the neutron reflection measurements and the DFG Schwerpunkt Polyelektrolyte (He 1616/7-4).

Appendix

To describe the scattering length density profile with a molecular model, we need to take each deposited polyelectrolyte layer into account:

$$\mathrm{SLD}(z) = v_{\mathrm{Si}}(z)\cdot\mathrm{SLD}_{\mathrm{Si}} + v_{\mathrm{H_2O}}(z)\cdot\mathrm{SLD}_{\mathrm{H_2O}} + v_{\mathrm{PAH}}(z)\cdot\mathrm{SLD}_{\mathrm{PAH}} + v_{\mathrm{PSS}}(z)\cdot\mathrm{SLD}_{\mathrm{PSS}} + v_{\mathrm{PSSd}}(z)\cdot\mathrm{SLD}_{\mathrm{PSSd}} \quad (A.1)$$

v_x describes the volume fraction of the respective molecules along the surface normal. As Figure 1 shows, the investigated polyelectrolyte multilayers consist of 18 different polyelectrolyte layers whose interpenetration we explore. The details of the molecular model are described in the following:

$z_0 = 0$ is the chosen as the position of the substrate/film interface, z_{18} corresponds to film/air interface. The internal interfaces are positioned at z_i, $i = 1, 2, ..., 17$.

Thus, we obtain for the substrate/film interface

$$v_{\mathrm{Si}}(z) = 1 - \mathrm{erf}\left(\frac{z - z_0}{\sigma_0}\right) \quad (A.2)$$

with a roughness $\sigma_0 = \sigma_{\mathrm{Si}}$. The error function is used to describe the profile,$\mathrm{erf}(z) = 1/\sqrt{2\pi}\int_{-\infty}^{z} e^{-t^2/2}\,dt$ (cf. Figure 6). The average water content α in the layer is given by

$$\alpha = \frac{N_{\mathrm{H_2O}}V_{\mathrm{H_2O}}}{N_{\mathrm{H_2O}}V_{\mathrm{H_2O}} + (V_{\mathrm{PSS}} + V_{\mathrm{PAH}})} \quad (A.3)$$

Since the water is homogeneously distributed across the polyelectrolyte multilayer, one obtains for its volume fraction

$$v_{\mathrm{H_2O}}(z) = \alpha\left[\mathrm{erf}\left(\frac{z - z_0}{\sigma_0}\right) - \mathrm{erf}\left(\frac{z - z_{18}}{\sigma_{18}}\right)\right] \quad (A.4)$$

The polyelectrolyte (PEI is assumed to have the same monomer volume and scattering length density as PAH) monomer fraction is parametrized as

$$v_{\mathrm{xxx}}(z) = (1 - \alpha)\cdot\sum_n\left[\mathrm{erf}\left(\frac{z - z_i}{\sigma_i}\right) - \mathrm{erf}\left(\frac{z - z_{i+1}}{\sigma_{i+1}}\right)\right], \quad i = 0, 1, 2, ..., 17 \quad (A.5)$$

since the polyelectrolyte layers extend from z_0 to z_1, z_1 to z_2, etc. Accordingly, the volume fractions of the polycation and of the nondeuterated and deuterated PSS layers are

$$v_{\mathrm{xxx}}(z) = \begin{cases} v_{\mathrm{PAH}}(z) & \text{for } i = 0, 2, 4, ..., 16 \\ v_{\mathrm{PSS}}(z) & \text{for } i = 1, 5, 9, 13, 17 \\ v_{\mathrm{PSSd}}(z) & \text{for } i = 3, 7, 11, 15 \end{cases} \quad (A.6)$$

The roughness between the respective layers is given by

$$\sigma_i = \begin{cases} \sigma_{\mathrm{Si}} + i(\sigma_{\mathrm{int}} - \sigma_{\mathrm{Si}})/4, & i = 0...3 \\ \sigma_{\mathrm{int}}, & i = 4...17 \\ \sigma_{\mathrm{f/a}}, & i = 18 \end{cases} \quad (A.7)$$

taking into account the gradual increase from the rather small Silicon/film roughness ($\sigma_{\mathrm{Si}} = \sigma_0 = 6$ Å, cf. Table 1) toward the internal roughness, σ_{int}, which is found to be at least a factor two larger. The scattering length density profiles are consistent with a gradual increase of the roughness between the first three adsorbed polyelectrolyte layers (cf. Figure 6).

Furthermore, to describe the scattering length density profile quantitatively, one has to account for the fact that the thickness of the three precursor and two outer layers differ from the one of the repeat units in the center of the multilayer. We assume a linear change in the thickness of the precursor and outer layers:

$$z_i = \begin{cases} 0, & i = 0 \\ z_{i-1} + f_i[2l_{\mathrm{precursor.av}} - l_{\mathrm{repeat.av}} + \frac{i}{2}(l_{\mathrm{repeat.av}} - l_{\mathrm{precursor.av}})], & i = 1...3 \\ z_{i-1} + f_i l_{\mathrm{repeat.av}}, & i = 4...16 \\ z_{i-1} + f_i[2l_{\mathrm{outer.av}} - l_{\mathrm{repeat.av}} + \frac{2}{3}(19 - i)(l_{\mathrm{repeat.av}} - l_{\mathrm{outer.av}})], & i = 17,18 \end{cases} \quad (A.8)$$

To calculate the interfaces between the different polyelectrolyte layers, we also take into account those different monomer volumes

$$f_i = \begin{cases} \frac{2V_{\mathrm{PAH}}}{V_{\mathrm{PSS}} + V_{\mathrm{PAH}}} = 0.66, & i = 1,3,5,...,17 \\ \frac{2V_{\mathrm{PSS}}}{V_{\mathrm{PSS}} + V_{\mathrm{PAH}}} = 1.33, & i = 2,4,6,...,18 \end{cases} \quad (A.9)$$

Note that $l_{\text{precursor.av}}$, $l_{\text{repeat.av}}$, and $l_{\text{outer.av}}$ are average values, not corrected for the different monomer volumes or the proximity to the interface. The film thickness corresponds to $d = z_{18}$. The three parameters $l_{\text{repeat.av}}$, $l_{\text{precursor.av}}$, and $l_{\text{outer.av}}$ can be directly calculated from Table 1 (with straightforward algebra).

References and Notes

(1) Decher, G. *Science* **1997**, *277*, 1232.
(2) Schönhoff, M. *Curr. Opin. Colloid Interface Sci.* **2003**, *8*, 86.
(3) Netz, R. R.; Joanny, J.-F. *Macromolecules* **1999**, *32*, 9013.
(4) Shiratori, S. S.; Rubner, M. F. *Macromolecules* **2000**, *33*, 4213.
(5) Clark, S. L.; Hammonds, B. *Langmuir* **2000**, *16*, 10206.
(6) Ahrens, H.; Büscher, K.; Eck, D.; Luap, C.; Papastavrou, G.; Schmitt, J.; Steitz, R.; Helm, C. A. *Macromol. Symp.* **2004**, *211*, 93.
(7) Lösche, M.; Schmitt, J.; Decher, G.; Bouwman, W. G.; Kjaer, K. *Macromolecules* **1998**, *31*, 8893.
(8) Schlenoff, J. B.; Dubas, S. T. *Macromolecules* **2001**, *34*, 592.
(9) Schmitt, J. Aufbau und strukturelle Charakterisierung von Multilagen aus Polyelektrolyten, Reaktivpolymeren und Kolloiden. Dissertation, Johannes Gutenberg-Universität, 1996.
(10) Dobrynin, A. V.; Rubinstein, M.; Obukhov, S. P. *Macromolecules* **1996**, *29*, 2974.
(11) Micka, U.; Holm, C.; Kremer, K. *Langmuir* **1999**, *15*, 4033.
(12) Kirwan, L. J.; Papastavrou, G.; Borkovec, M.; Behrens, S. H. *Nano Lett.* **2004**, *4*, 149.
(13) Büscher, K.; Ahrens, H.; Graf, K.; Helm, C. A. *Langmuir* **2002**, *18*, 3585.
(14) Als-Nielsen, J. Solid and liquid surfaces studied by synchrotron X-ray diffraction. In *Structure and Dynamics of Surfaces*; Blanckenhagen, W. S. a. W., Ed.; Springer: New York, 1986.
(15) Pedersen, J. S. *J. Appl. Crystallogr.* **1992**, *25*, 129.
(16) Pedersen, J. S.; Hamley, I. W. *J. Appl. Crystallogr.* **1994**, *27*, 36.
(17) Daillant, J.; Gibeau, A. *X-ray and Neutron Reflectometry: Principles and Applications*; Springer: Berlin, 1999.
(18) Asmussen, A.; Riegler, H. *J. Chem. Phys.* **1996**, *104*, 8159.
(19) Tan, H. L.; McMurdo, M. J.; Pan, G. Q.; van Patten, P. G. *Langmuir* **2003**, *19*, 9311.
(20) Chodanowski, P.; Stoll, S. *J. Chem. Phys.* **1999**, *111*, 6069.
(21) Waigh, T. A.; Ober, R.; Willimas, C. E.; Galin, J. C. *Macromolecules* **2001**, *34*, 1973.
(22) Goerigk, C.; Schweins, R.; Huber, K.; Ballauf, M. *Europhys. Lett.* **2004**, *66*, 331.
(23) Steitz, R., Jaeger, W.; von Klitzing, R. *Langmuir* **2001**, *17*, 4471.

MA047552C